Evaluation of the Transfer Coefficient Matrix (TCM) approach to model the atmospheric radionuclide air concentrations from Fukushima

Roland R. Draxler[1] and Glenn D. Rolph[1]

Received 21 November 2011; revised 6 January 2012; accepted 9 January 2012; published 6 March 2012.

[1] A procedure is developed and tested to provide operational plume forecasts in real-time by continuously updating the previous day's simulations as new meteorological data become available. Simulations are divided into smaller time segments and each segment is continued as an independent calculation using a unit source emission. Multiple computational species are tracked at the same time to represent different classes of radionuclides, each with different dry and wet deposition characteristics. When quantitative air concentration results are required, the unit source calculations are multiplied by the appropriate temporally varying emission rates and decay factors for the radionuclide species involved. Air concentrations for multiple emission scenarios can easily be created in a few minutes and used to optimize model results as more measurement data become available. The procedure was evaluated for the Fukushima accident using publically available emission estimates and some I-131 and Cs-137 monitoring data. The model performance was evaluated at four sampling locations (Dutch Harbor, Alaska; Seattle, Washington; Dublin, Ireland; and Huelva, Spain) at various distances from Japan. The model results showed a very high correlation for the I-131 particulate predictions (0.94) and a moderate correlation for the Cs-137 predictions (0.40). The cesium predictions at Seattle showed five distinct time periods of concentration over-predictions associated with two peak emission periods. Adjusting these emission rates downward to correspond more closely with the time-adjacent rates eliminated the over-prediction but resulted in total emissions of Cs-137 (3 PBq) that were much less than estimated by other researchers (36 PBq).

Citation: Draxler, R. R., and G. D. Rolph (2012), Evaluation of the Transfer Coefficient Matrix (TCM) approach to model the atmospheric radionuclide air concentrations from Fukushima, *J. Geophys. Res.*, *117*, D05107, doi:10.1029/2011JD017205.

1. Introduction

[2] The provision of plume dispersion products in rapidly evolving emergency response scenarios frequently relies upon a class of 3-dimensional particle models identified by the term Lagrangian, which refers to the computational approach in solving the dispersion equations only in the vicinity of the pollutant plume rather than over the entire meteorological data grid. This reduced computational domain generally provides faster results than other approaches. However, at longer distances from the release point the particle density may not be sufficient to describe the pollutant plume distribution, which then requires the release of many more particles, putting an additional burden on computational resources. The intent of this analysis is to re-examine the computational approach to determine if there are other ways to apply Lagrangian techniques to the very long-range dispersion problem and still provide robust predictions quickly.

[3] The National Oceanic and Atmospheric Administration (NOAA) uses a Lagrangian model to provide long-range plume forecasts [*Draxler et al.*, 1997] to World Meteorological Organization (WMO) Member States in its region (North, Central, and South America) and the International Atomic Energy Agency (IAEA) when requested. As part of an agreement with the WMO, NOAA acts as one of their eight Regional Specialized Meteorological Centers [*WMO*, 2006, 2010]. An RSMC would be designated as the primary center to provide products to the IAEA if the incident occurs in their region of responsibility. Several of the other WMO modeling centers also use Lagrangian models (Canada [*D'Amours et al.*, 2010]; United Kingdom [*Jones et al.*, 2007]; Australia and China, who use the same model as NOAA).

[4] The release of radioactive materials from the Fukushima Daiichi Nuclear Power Plant resulting from the Great Earthquake and Tsunami of March 2011 provided many operational challenges in modeling their atmospheric transport, dispersion, and scavenging. Besides the obvious uncertainties in determining what and how much was released to the atmosphere, uncertainties in the various removal processes that occur, such as gravitational settling of particles and the

[1]NOAA Air Resources Laboratory, Silver Spring, Maryland, USA.

This paper is not subject to U.S. copyright.
Published in 2012 by the American Geophysical Union.

scavenging by precipitation, can lead to large uncertainties in the predicted downwind concentrations.

[5] During the incident, because the emissions were continuing, the operational procedure was to produce a new forecast each day. As a result of previously agreed upon procedures as defined by *WMO* [2010], the default simulation assumed a unit source emission for six hours then calculated 24-h time integrated air concentrations and deposition for the next 72 h. However, previous emissions were not continued into the forecast period and eventually later in the incident, as more detailed emission estimates became available, it became impractical to rerun the entire simulation from the beginning of the emission period.

[6] In this analysis, we examine the feasibility of implementing a variation of the above operational procedure that would be more flexible in responding to changing conditions and input data. The method involves running each user defined emission period, in our example assumed to be six hours, as an independent calculation using a unit source emission rate, as long as releases to the atmosphere continue. All previous release period calculations are updated to the current time as new meteorological data become available, and the calculations can then be continued into the forecast period if desired. The underlying principle is that the atmospheric phenomena (transport, dispersion, scavenging) for any given species are completely independent of the actual source's emissions of that species. The transport, dispersion, and atmospheric fate aspects of the calculation are the most time consuming calculation, but they only need to be done once. This contrasts with more traditional simulations, where the time-varying source term is specified, and the atmospheric simulation directly outputs the air concentration predictions.

[7] Air concentrations are calculated in a post-processing step. The unit source calculations give the dispersion factors from the release point for every emission period to each downwind grid location, defining how much of the emissions are transferred to each location varying as a function of time, which is defined here as the Transfer Coefficient Matrix (TCM). The TCM is computed for inert and depositing species and the final air concentration is computed in a simple post-processing step by multiplying the TCM by the appropriate emission rate and radioactive decay constant. The contribution of each release time to the concentration at any receptor location can also be computed resulting in an interactive process to minimize the difference between model predictions with any available measurement data while adjusting the emissions for the relevant time periods.

[8] The TCM concept is not new; it was first applied at NOAA to compute a dispersion climatology [*Draxler and Heffter*, 1981]. More recently, unit-source time and height varying simulations were conducted by *Stohl et al.* [2011a] to estimate the ash emissions from the Eyjafjallajökull eruption and especially relevant to this analysis, to estimate the Xenon-133 and Cs-137 releases from Fukushima [*Stohl et al.*, 2011b]. The concept is expanded here to address how it can be applied to real-time simulations and the types of information that can be extracted from a TCM.

2. Model Design

[9] The calculation of the transport and dispersion from the source was done using the Hybrid Single-Particle Lagrangian Integrated Trajectory (HYSPLIT [*Draxler and Hess*, 1998]) model. In HYSPLIT, the computation is composed of four components: particle transport by the mean wind, a turbulent transport component, scavenging and decay, and finally the computation of the air concentration. A large number of pollutant particles (by convention called "particles" but that are computational "point" entities that may be particles or gases), are released at the source location each time step and passively follow the wind. The mean particle trajectory is the integration of the particle's position vector in space and time. The turbulent component of the motion defines the dispersion of the pollutant cloud and is computed by adding a random component to the mean advection velocity in each of the three-dimensional wind component directions. The vertical and horizontal turbulence is computed from the local stability estimated from the wind and temperature profiles. Air concentrations, or dispersion factors in this case, are computed by summing each particle's mass (or activity for radiological emissions) as it passes over a concentration grid cell and dividing the result by the cell's volume. A detailed description of the computational aspects of the model is given by *Draxler and Hess* [1997] and its configuration is reviewed by *Draxler* [1999].

[10] The TCM modeling approach was tested in its proposed operational configuration, but post-event, using analyzed meteorological fields. A new simulation was started every six hours, with an emission rate of one unit/hr for a duration of six hours for each simulation segment. The calculation segments are updated until the end of the incident. Every six hours the number of segments increases by one. The transfer coefficients, essentially air concentrations resulting from the unit emission rate, are also computed as six hour averages, output every six hours. The resulting TCM is of the form,

$$\mathrm{TCM}_{i,j,k} \tag{1}$$

where i represents the number of time varying releases, j represents the number of sampling periods available over k grid points. If desired, simulations could also be conducted for multiple release heights, adding an additional element to the array. As time increases with each new release (i), there will be one less output period (j). For the Fukushima example discussed in more detail in the next section, the calculation was started on 11 March and continued through 20 April, a duration of 41 days, which means that when new simulations are started at 6 h intervals (4 per day), 164 simulations are running at the end of the computational period. The first release would contain 164 output periods (j) while the second release would have 163 output periods. The entire simulation consists of 13,530 computational segments {j (j + 1)/2}.

[11] In the post-processing step, a constant emission rate (Q) is defined for each 6-h emission period, and therefore the air concentration (C) becomes

$$C_{j,k,m} = \sum Q_{i,m} D_m \mathrm{TCM}_{i,j,k,m}, \tag{2}$$

where D is a species (m) dependent radioactive decay factor and the sum is taken over all release time periods (i). The product $Q_{i,m}$ $\mathrm{TCM}_{i,j,k,m}$ shows the contribution of each release to the total predicted concentration at the sampling time (j), at location indices (k), and for the computational

species (m). A computational species may represent one or more radionuclides.

[12] One critical aspect for quantitative predictions of air concentration is the wet and dry scavenging that occurs along the transport pathway. The computational details are given in Appendix A. Four generic species were tracked as surrogates for the radionuclides: a gas with no wet or dry scavenging, a gas with a relatively large dry deposition velocity (0.01 m/s) and wet removal (Henry's constant = 0.08, from R. Sander, Compilation of Henry's law constants for inorganic and organic species of potential importance in environmental chemistry, Version 3, 1999, http://www.rolf-sander.net/henry/) to represent gaseous I-131, a particle with a small deposition velocity (light particle 0.001 m/s), and a particle with a larger deposition velocity (heavy particle 0.01 m/s). There can be considerable variability in scavenging coefficients [*Lindberg*, 1982] and the wet scavenging coefficients used in these calculations are lower than the original model default values [*Draxler and Hess*, 1997; *Hicks*, 1986] but these lower values are consistent with the results from more recent deposition studies [*Cohen et al.*, 2002] using the HYSPLIT scavenging parameterizations.

[13] In the post-processing step the species must be selected and assigned to a computational species in the TCM. For instance Cs-137 and particulate I-131 would be assigned to the light particle, while gaseous I-131 has its own TCM. Most other particulate species could be assigned to either the light or heavy particle class. If the desired species does not have a suitable existing computational surrogate, then the TCM must be recomputed with the additional species' scavenging characteristics. Radioactive decay is applied for each species from the time of the reactor shutdown in the post-processing step, not during the TCM computation. At this stage, only decay, not in-growth is included in the calculations.

3. Accident Scenario

[14] The details of the earthquake, tsunami, and Fukushima Daiichi Nuclear Power Plant failures resulting in radioactive emissions to the atmosphere and adjacent waters have been extensively documented by the Science Council of Japan (http://www.scj.go.jp/en/index.html). To briefly summarize the time-line of critical events, the earthquake occurred on March 11th at 14:26 Japan Standard Time (JST), the tsunami about one hour later at 15:41, and by 16:36 a nuclear emergency was reported. By the early morning hours of March 12th, the pressure in the containment vessel of Unit 1 began to rise and around 04:00 the condenser stopped operating. This is the point at which the Nuclear Safety Commission (NSC) estimated that the atmospheric emissions started (chapter II, p. 389, http://www.meti.go.jp/english/earthquake/nuclear/iaea/iaea_110911.html). JST is +9 h from Greenwich, which puts the release start at 19:00 UTC on March 11th. Subsequently all times discussed will be in UTC.

3.1. Emissions

[15] We used a preliminary estimate of the temporal emission variation based upon model estimates and back-calculations from air concentration measurements as reported by *Chino et al.* [2011] which showed a total emission of 1.5×10^{17} Bq I-131 and 1.3×10^{16} Bq Cs-137 from 11 March through 5 April. Emissions for the first few days (11–15 March) were subsequently updated by the NSC (chapter II, p. 400, http://www.meti.go.jp/english/earthquake/nuclear/iaea/iaea_110911.html), and these new values were used for our initial releases for I-131, resulting in a total emission of 1.3×10^{17} Bq I-131 and 7.6×10^{15} Bq Cs-137 from 11 March through 5 April. These values are close to the totals reported by the Nuclear and Industrial Safety Agency (NISA) and the Japan Nuclear Energy Safety Organization (JNES) of 1.3×10^{17} Bq I-131 and 6.1×10^{15} Bq Cs-137 as reported by the NISA press release of 12 April 2011 (http://www.nisa.meti.go.jp/english/files/en20110412-4.pdf). The emission time series used in our calculations is shown in Figure 1. There is considerable uncertainty surrounding the emission totals as well as its more detailed temporal variation. However, one of the primary advantages of our TCM approach is that different emission scenarios can easily be applied and the difference between the resulting air concentrations and observations can be minimized.

[16] One other required piece of model input information is the partitioning of the I-131 releases between the particulate and gas phase. *Morino et al.* [2011] assumed that 80% of the emissions were in the gas phase. *Masson et al.* [2011] reported that measurements taken near Fukushima showed that the average ratio of gaseous to total I-131 was around 0.71 and that their European measurements showed an average gaseous to total I-131 ratio of 0.77. *Masson et al.* [2011] expected a slight increase of the ratio with time because the particulate I-131 will be removed more efficiently by scavenging and suggested that the relative stability of the ratio with time meant that little of the gaseous I-131 was converted to particulate form during transport. *Moyers and Duce* [1972] found a similar partition in non-radioactive forms of iodine, reporting that gaseous iodine concentrations were 2 to 4 times larger than particulate iodine in the marine atmosphere, where a factor of three results in a ratio of 0.75. The gas-particulate partition is a complicated issue, and for our initial calculations we assumed 0.7, a value at the lower end of the reported range with no gas-particle conversions during transport.

3.2. Sampling Data

[17] Various radionuclide measurement data related to Fukushima are starting to appear in the literature [*Masson et al.*, 2011; *Manolopoulou et al.*, 2011; *Bowyer et al.*, 2011]. Perhaps eventually there may be a central repository of monitoring data available to the scientific community, but for now we have focused on four sampling locations: Dutch Harbor, Alaska (53.9N 166.5W), which is part of the U.S. Environmental Protection Agency's radiological sampling network (RADNET, http://www.epa.gov/japan2011/rert/radnet-sampling-data.html); Seattle, Washington (47.7N 122.4W) as reported by *Leon et al.* [2011], Dublin, Ireland (53.4N 6.2W), from the Radiological Protection Institute of Ireland (http://www.rpii.ie/Documents/Monitoring/Fukushima/fukushima-air-monitoring.aspx), and at Huelva, Spain (37.3N 6.9W), as reported by *Lozano et al.* [2011]. Most samples were of one or more days duration and we only focused upon the measurements of I-131 and Cs-137. The EPA used filter packs to collect particulate species and activated charcoal canisters to collect the gaseous species. Only particulate species measurements were available at Seattle, Dublin,

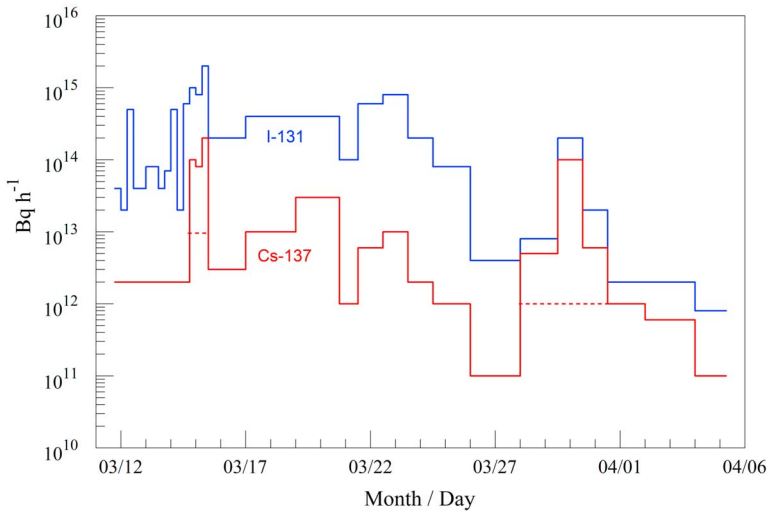

Figure 1. Time-varying hourly emission rates shown as 6-h averages for Cs-137 (red) and total I-131 (blue) as adapted from *Chino et al.* [2011]. The dashed line shows the modified source based upon the results from the TCM calculation.

and Huelva. Although there may be considerable uncertainties associated with various radiological measurements, this issue is not critical for the interpretation of the TCM results.

3.3. Simulation Configuration

[18] The basic dispersion calculation to create the TCM used a 3-dimensional particle approach by releasing 5,000 particles per hour over the 6-h duration of each segment. Therefore, each release time period consisted of following 30,000 particles. The particle release rate we used is on the low end of the acceptable range. Higher particle release rates are desirable if computational resources are available. When the particles from this release are updated with the next six hours of meteorology, no additional particles are released, but a new segment is started for the emissions during that period. At the end of the computation (20 April), a total of 4,920,000 particles were being tracked by 164 independent simulations. This approach lends itself easily to parallel computing, where each simulation can be made on its own processor independent of all other calculations until the air concentrations are computed. All test calculations were run on a Xeon E5540 1.596 MHz processor taking about two minutes for each 6-h computational segment. As noted earlier, there were 164 releases tracked at the end of the simulation period, which means that a six-hour update would take about five hours on one processor. Adding together the TC values from all the simulations to compute the total air concentration only takes a few minutes.

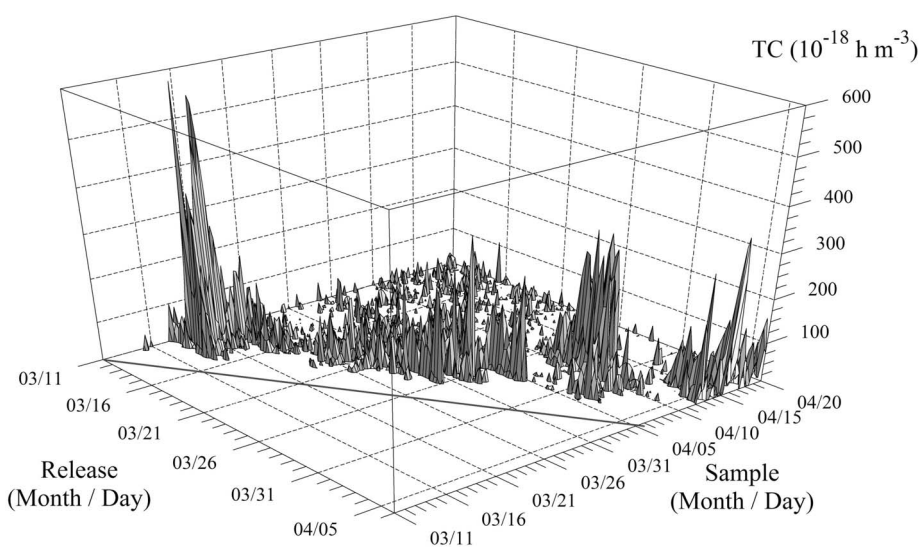

Figure 2. The transfer coefficient matrix without dry/wet removal or radioactive decay computed for Seattle, Washington. Along the 1:1 diagonal line, emission time = sampling time; thus the distance along the sampling axis from the diagonal line to the first nonzero sample represents the minimum travel time from source to receptor.

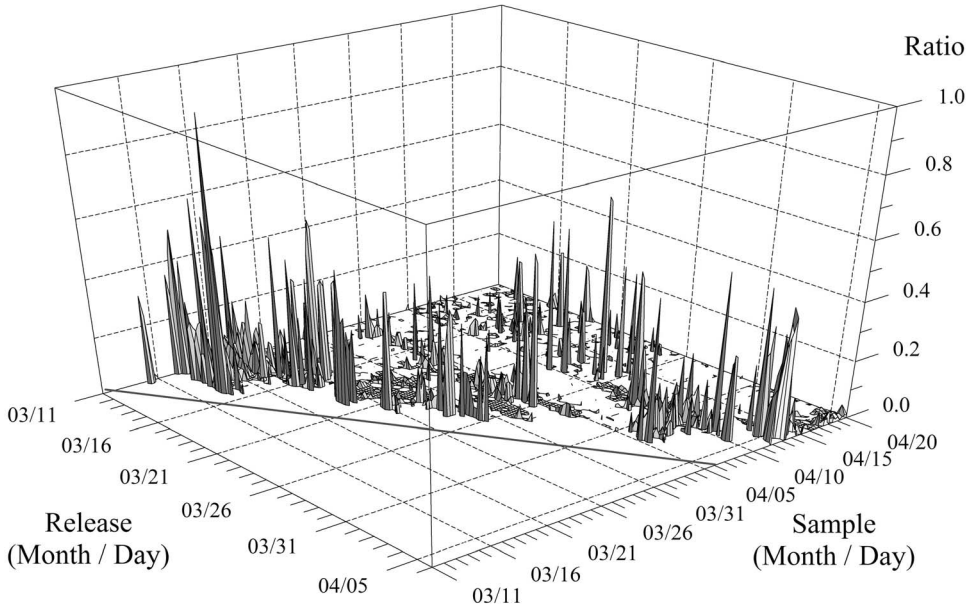

Figure 3. The ratio of the depositing to non-depositing transfer coefficients at Seattle. A value of one indicates that no deposition occurred between the time that the pollutant was released at the source and collected at the sampler.

[19] All calculations used the 0.5-degree horizontal resolution meteorological data from NOAA's Global Forecast System (GFS), consisting of a series of 0 to +6 h forecasts available on GFS native model sigma levels (56) with meteorological fields available every three hours. The concentration grid was global at 1-degree horizontal resolution with a vertical extent of 500 m. The TCM values were computed as the sum of all particles in each grid cell divided by its volume. The relatively coarse resolution concentration grid compared to the meteorology grid permits the release of fewer particles. The resolution of the meteorology and concentration grids is not appropriate for examining concentrations near the source; however it is quite suitable for the long-range transport from Japan to the United States and Europe.

4. Transfer Coefficient Matrix

[20] To illustrate the results of the TCM calculation, the transfer coefficients (TC) extracted for the grid point over the Seattle sampler for the entire computational period are shown in Figure 2. The vertical axis shows the TC without any scavenging or radioactive decay, the left axis is the time of the release, and the right axis is the sampling time. The plot shows the TC in discrete six hour intervals. The distance from the blue diagonal line parallel to the sampling axis is the travel time that it took for each release to show a value at the sampler. Peak TC values of 600×10^{-18} h m^{-3} occur for the samples around 20 March, which resulted from the releases around 12–13 March. Multiplication of this TC value by the release rate for Cs-137 of 2×10^{12} Bq h^{-1} (Figure 1) would result in an air concentration of about 0.001 Bq m^{-3}. This would be the maximum concentration one would expect if the cesium was not subject to any decay, nor wet or dry scavenging. This concentration only represents the contribution from one release. The total predicted concentration at that time would be computed from the sum of the TC over all the sources for that sample time.

[21] The TCM provides additional quantitative information. For instance, there are four periods when the transport is favorable (high TC values) to the sampling site: March 20, April 10, April 18, and to a lesser extent March 29 through April 4. The depth of the high TC values along the sampling axis indicates that the plume duration from any one release might last as much as five days. The fact that the peak TC values follow a diagonal parallel to the emissions line, shows that typical transport times range from 5 to 10 days and the plume might linger for another 5 days. This suggests that future modeling efforts can be simplified by dropping particles from the computation after perhaps 20 days, if the interest was only in samples collected near Seattle.

[22] After the initial plume impact, very small signals can persist for quite some time, such as shown in April for the initial releases in March, which are most likely due to individual particles randomly impacting the sampling location after completing a more indirect path from the source to the sampler, perhaps even the result of a global transit. Depending upon the time- and space-varying winds, plume segments from successive releases may not reach the sampler in the same sequence. For instance, the releases from April 1 arrived at the sampler around April 6–10, much earlier than the releases from 30 March, which did not arrive until around 9 April.

[23] To illustrate the effects of scavenging (without radioactive decay), the ratio of the TC of a light particle to the non-depositing TC is shown in Figure 3, defined here as the TC ratios (TCR). There are no TCR values near one because even during transport situations with no precipitation, the particles are subject to dry deposition, continuously removing a small fraction of mass from the layer near the ground. Also illustrated here is that atmospheric scavenging is very effective in removing much of the later contributions

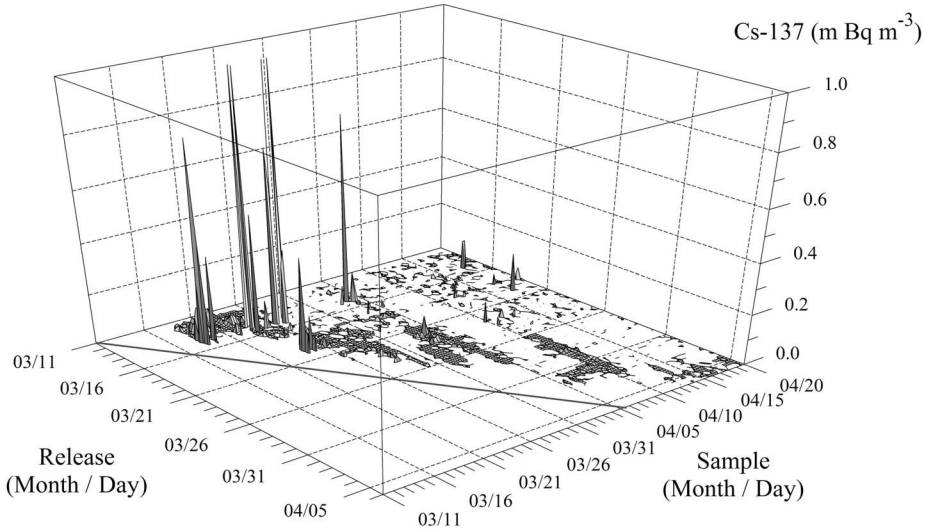

Figure 4. Concentrations of particulate cesium at Seattle shown by date of release and the sample date. Adding all the values along the release axis for a particular sample date would result in the total model predicted value for that period.

to the sampler after the initial plume impact from any one release, because the greater the transport time the more removal can take place.

[24] Some of the particles making small contributions as shown in Figure 2 have probably taken some very circuitous routes to arrive in Seattle. The many isolated small peaks further downstream (in time) of the main diagonal are still associated with a very small TC, but the high TCR indicates that those particles were not subjected to much scavenging during their transport. With respect to the previously

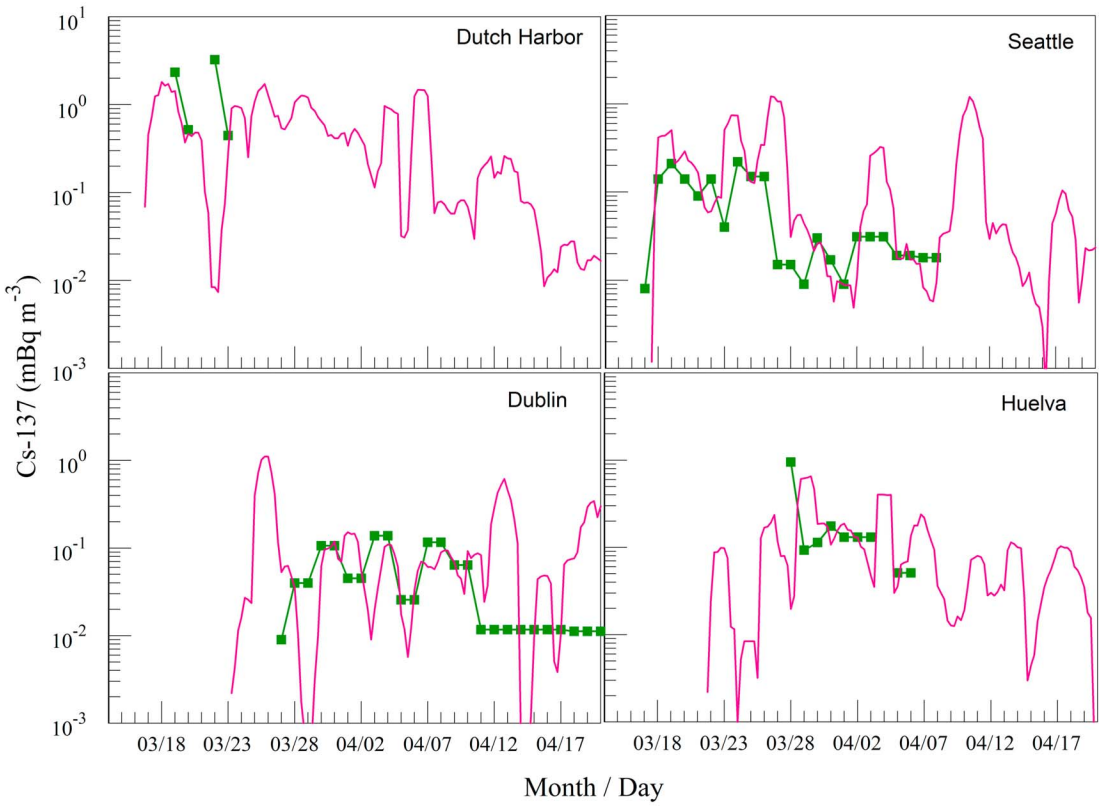

Figure 5. The concentration time series for Cs-137 at four sampling locations using the emission rates indicated by the solid red line shown in Figure 1. Measurements are shown in green, and the solid red line is the model prediction.

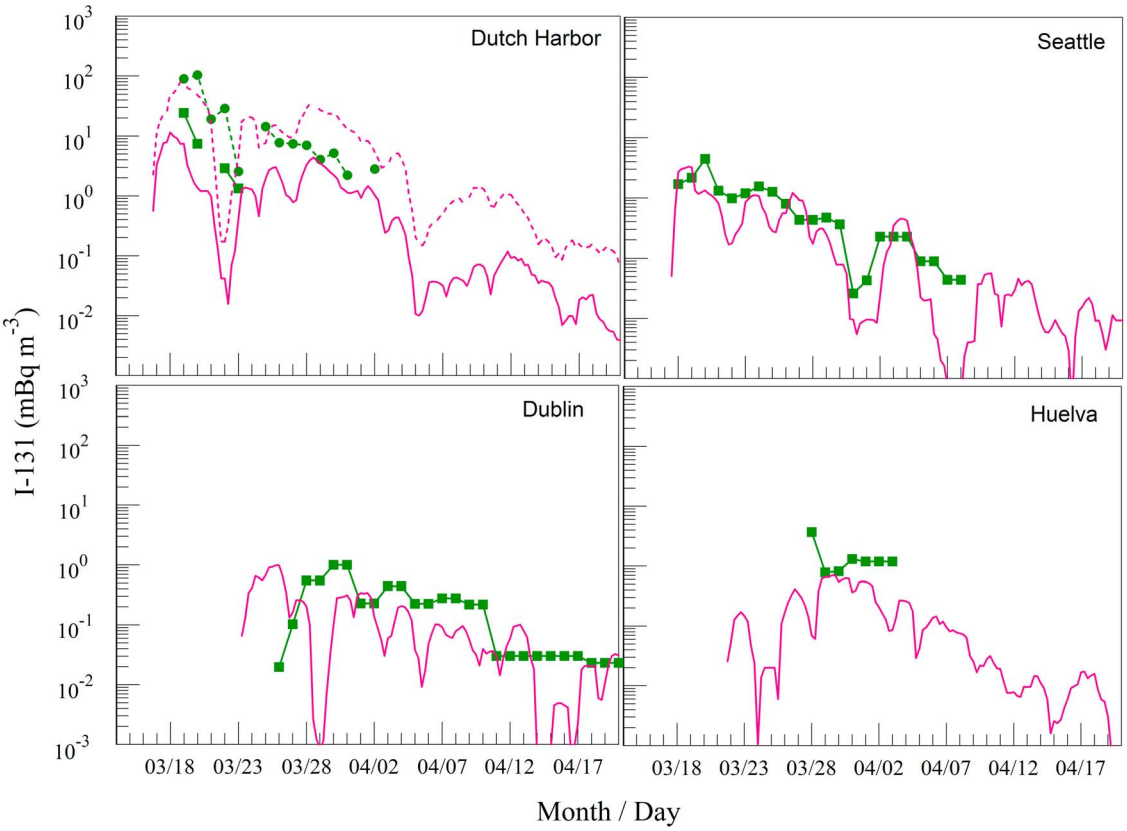

Figure 6. The concentration time series for particulate I-131 (green squares, measured data; solid red line, model prediction) at four sampling locations using the emission rates indicated by the solid blue line shown in Figure 1. The Dutch Harbor site also shows the gaseous iodine (green dots, measured values; dashed red line, the model prediction).

identified periods with high TC values, the impact of these has been considerably reduced, especially the periods in April. Low TCR values do not mean low air concentrations, but that the air concentration will be very sensitive to the scavenging that occurs during transport. However, because the scavenging is one of the most sensitive aspects of the calculation, there will be more uncertainty associated with the predicted concentrations for those samples.

[25] The last step in processing the TCM is to apply a time-varying source term and radioactive decay to obtain the air concentrations. This is shown in Figure 4 for particulate Cs-137. Here we see the effects of high emissions during the initial period of the accident, modulated by both scavenging and decay, generally resulting in very small concentrations after the initial plume impact. Also, due to the time-varying nature of the source, some of the TC peaks shown in Figure 2 no longer appear (although the atmospheric transport may have been very direct, the emissions were much smaller). One interesting result shown here is how the releases from 14 to 15 March persisted in four distinct peaks until 5 April. This will be examined in more detail in section 6.

5. Model Application

[26] The time series of air concentrations was extracted from the TCM (the integral along the release axis of Figure 4) using the emission rates shown in Figure 1 (solid lines) at the four sampling stations selected for their varying distance from Japan. The Cs-137 results are shown in Figure 5. The six-hour duration model estimates were averaged into 24-h periods to correspond with the sampling data. Although there is a lot of variability in the model predictions, presumably from differences in the wet scavenging between releases (Figure 3), the large scale peaks and troughs seem to have some correspondence with the trends in the measurements. The correlation between the predictions and measurements over all samples at the four sites is 0.40 with the average calculated and measured values of 0.19 and 0.18 mBqm^{-3}, respectively, for the predictions that have a corresponding measurement.

[27] The high model predicted cesium values in mid-April at Seattle and Dublin seem suspicious and may be due to inaccurate emission estimates. The concentration predictions can easily be adjusted by determining the date of the releases (late March, early April) corresponding to the over-predictions and re-computing the air concentrations with a different emission estimate. However, the magnitude of the scavenging may be just as important in predicting the air concentration as determining the correct emissions. For this period, Figure 3 shows relatively high ratios for sources contributing to the 10–11 April samples, suggesting that scavenging did not play a significant role and that the concentration over-prediction could be reduced by decreasing the emissions (or increasing the scavenging).

[28] The corresponding I-131 results are shown in Figure 6. First, the particulate iodine was treated computationally the same as cesium and the model shows a comparable performance in terms of matching the large scale feature in the individual measured time series. Although there is evidence of some under-prediction, visually, the results look much better than the cesium predictions, but this is in part due to the fact that the concentration range between the smaller scale peaks and troughs is much less for iodine than cesium. Both predictions used the same TCM values to compute air concentrations. The correlation between the predictions and measurements over all samples at the four sites is 0.94 with the average calculated and measured values of 0.65 and 1.63 $mBqm^{-3}$, respectively.

[29] As mentioned earlier, the computation is based upon an assumption regarding the initial partition of the I-131 release into gases and particles. The gaseous I-131 predictions at Dutch Harbor, although very noisy, are of comparable magnitude with the measurements (Figure 6), while the particulate predictions are slightly lower than the measurements, consistent with the I-131 particulate predictions at the other locations. This result suggests that either the particulate I-131 scavenging should be less than the Cs-137 scavenging, or there might be processes occurring during transport affecting the gas-to-particle conversions, or the initial partition of the I-131 emissions should put less into the gas phase. This latter assumption was easily tested by re-computing the air concentrations using a different partition. Using an initial value of 50% for the I-131 emissions, the model predicts a gas to total I-131 ratio over Europe of 0.78, comparable to the value reported by *Masson et al.* [2011]. This result only provides some circumstantial evidence and we really do not know for certain which process is the most important in determining the downwind I-131 concentrations.

6. Discussion

[30] The primary difference between an explicit plume simulation and the TCM approach outlined here is that the former requires knowledge of the temporal variation in emissions prior to running the transport and dispersion calculation, while in the TCM method the emission rates are applied after the dispersion calculation has completed. If the emission rate were constant with time, then there would be no advantage to the TCM approach as the concentrations from the plume calculation can easily be adjusted by the difference in the emissions without re-running the complete model simulation. However, the emissions from Fukushima had quite large variations in time.

[31] An example of how the emissions can be adjusted using the TCM can be demonstrated for the Cs-137 measurements, which showed many over-predicted peaks. The large modeled cesium peak shown at Seattle (Figure 5) around 10–11 April, and discussed previously, appears after the measurements were all below the detection threshold. Examining the TCM (Figure 2 or Figure 4) for those days indicates that although many different emission times contributed to those samples, emissions between 27 March to 1 April were the primary contributors. The estimated emissions (Figure 1) show a substantial increase during that period. In contrast, the four remaining large over-prediction peaks, 19 March, 24 March, 27 March, and 3 April, all seemed to be associated with emissions from a single time period, around 15 March (Figure 4), a time period also associated with a large increase in emissions. If we assume that the emissions did not increase, but remained at the about the same level (dashed line in Figure 1) for both of these periods and recalculate all the air concentrations, the results, shown in Figure 7, indicate a substantial improvement at Seattle, Dublin, Dutch Harbor, and Huelva. The two April cesium peaks still seems a little high, but considering the scavenging uncertainties, and the fact that the TCR is high (Figure 3), suggests that although the emissions were important, more wet scavenging may be required for these events. In the current modeling framework it is much easier to adjust the emissions for a specific time period than the scavenging.

[32] At this point we have only examined the concentration over-prediction, as these cases were apparently associated with increased emissions. Although there is much uncertainty in the temporal variation of the emissions, we know that they were continuous within a certain order-of-magnitude range. This same restraint does not apply to the scavenging, because there is no lower limit to the predicted air concentrations subjected to wet removal. For example, consider the minimum predicted concentration at Seattle (Figure 7) occurring on 16 April. That period is also associated with a very low TCR, suggesting a lot of scavenging must have occurred along the transport path. Because the measurements were below the detection limits at this time, it is not possible to make a quantitative adjustment. However, it is clear that increasing the emissions by multiple orders-of-magnitude to raise the predictions to levels consistent with the surrounding values, would be outside of an acceptable adjustment range and the very low predicted air concentrations can only be due to an over-estimation of the scavenging.

[33] In this analysis we applied a simple qualitative approach to adjusting the emissions to demonstrate the utility of the TCM and the TCR was only used in the interpretation of the model predictions. Because the computation of air concentration from the TCM is linear (the contributions from each release can be added together), the source adjustment can be performed in a more quantitative manner, through the minimization of a cost function (the difference between the model predictions and measurements) from a first-guess solution such as described by *Seibert* [2000]. In this type of approach, it is possible to introduce the TCR as a weighting function to constrain the solution to those periods when the scavenging had less influence on a particular source-receptor pairs.

[34] Although the qualitative corrections to the Cs-137 emissions discussed above provided a better fit with the measured data, the results are inconsistent with some of the recently published results [*Stohl et al.*, 2011a, 2011b]. They found that the total Cs-137 emissions were almost three times larger (36×10^{15} Bq versus 13×10^{15} Bq) than those determined by *Chino et al.* [2011]. The adjusted Cs-137 emissions (dashed line in Figure 1) that provided the relatively good comparison with the measurements shown in Figure 7, represent a total Cs-137 emission of only 3×10^{15} Bq. Although *Stohl et al.* [2011a, 2011b] attributed an uncertainty to their estimate of 67% to 150%, our results fall

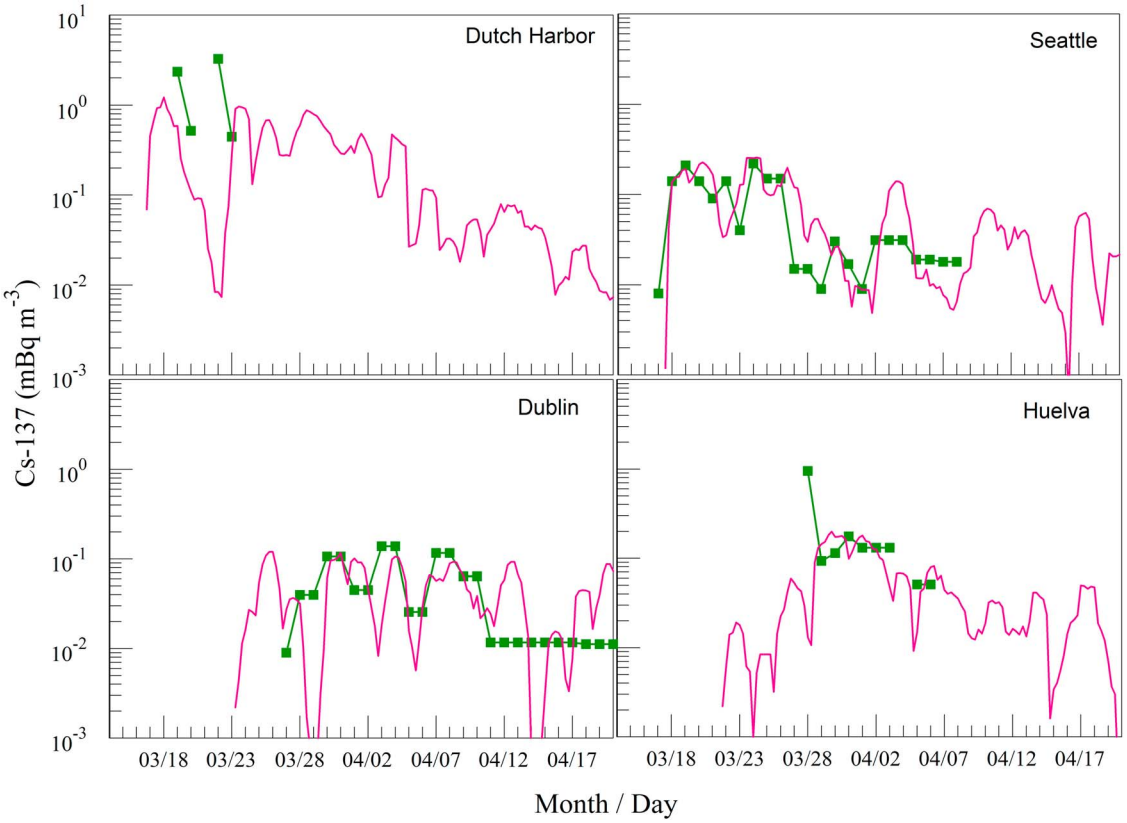

Figure 7. As in Figure 5, but the model predictions for Cs-137 use the adjusted source term (dashed line replaces solid line in Figure 1).

well below that range. There are huge uncertainties in estimating the source term from air concentration measurements and dispersion model predictions, primarily related to wet scavenging (precipitation fields as well as removal coefficients). For instance, the greater the precipitation scavenging by the transport-dispersion model, the greater the emissions need to be for the calculation results to match the measurement data. These issues may never be completely resolved even after observed precipitation fields and higher spatial- and temporal-resolution meteorology are introduced into the transport-dispersion model calculations.

7. Summary

[35] We presented a technique that can easily be applied in an operational environment to quickly calculate pollutant plumes when detailed real-time source information is not available. The transport and dispersion component of the prediction using a unit source emission rate is computed in discrete time segments. The calculations can be updated as the event progresses, including appending forecasts, started from the archived calculations. The computational results are saved as a transfer coefficient matrix so that the contribution of each release segment can be identified in all the sampling periods. A time varying emission rate is then applied to each source vector in the matrix. As more detailed source information becomes available, or measurement data become available, the time varying emissions can be adjusted to improve the match with the measured data without re-computing the transport and dispersion, which may involve a considerable cost in computer resources requiring the tracking of millions of particles. The matrix can be analyzed in the traditional way by integrating all the emissions for a specific sampling period to compute the total predicted concentration, or by extracting the time-varying contribution from each emission period to a specific sample. The latter technique can be used to optimize the temporal variation of the emission rates. The computational technique was demonstrated for the releases from the Fukushima NPP. An interactive version of this analysis is online (http://ready.arl.noaa.gov/READY_fdnpp.php) and can be used to extract the model predictions for other locations, species, and temporal emission profiles.

Appendix A: Computation of Scavenging and Deposition

[36] In HYSPLIT, wet scavenging is parameterized through removal constants β (s^{-1}), where the deposition D over time step Δt for each particle of mass M is

$$D = M\{1 - \exp[-\Delta t(\beta_{dry} + \beta_{gas} + \beta_{inc} + \beta_{bel})]\}. \quad (A1)$$

[37] The particle mass is reduced by D each time step. The time constant for within-cloud removal for particulate pollutants is

$$\beta_{inc} = S P \Delta Z_p^{-1}, \quad (A2)$$

where S is the ratio of the pollutant's concentration in water to its concentration in air (4×10^4), ΔZ_p is the depth of the pollutant layer, and the precipitation rate P is the value predicted by meteorological model used in the calculation. Below-cloud removal is defined directly as a rate constant ($\beta_{bel} = 5 \times 10^{-6}$), independent of the precipitation rate. The wet deposition of gases depends upon their solubility and for inert non-reactive gases it is a function of the Henry's law constant (H - Molar atm^{-1}), the ratio of the pollutant's equilibrium concentration in water to that in air. Therefore, the gaseous wet removal time constant is

$$\beta_{gas} = \mathrm{H\,R\,T\,P}\,\Delta Z_p^{-1}, \tag{A3}$$

where R is the universal gas constant (0.082 atm M^{-1} K^{-1}), T is temperature, and the wet removal of gases is applied at all levels from the ground to the top of the cloud-layer. The dry deposition calculation is limited to particles within the surface layer (ΔZ_p is usually about 75 m), and the time constant is

$$\beta_{dry} = V_d\,\Delta Z_p^{-1}. \tag{A4}$$

[38] Although radioactive decay, by itself, does not result in deposition, airborne and deposited radioactive pollutants do decay, and hence the airborne particle mass and deposition amounts are adjusted for radioactive decay each time step also using the time constant approach

$$\beta_{rad} = \ln 2/T_{1/2}, \tag{A5}$$

where the decay constant for radioactive processes is defined by the half-life ($T_{1/2}$).

[39] **Acknowledgment.** We wish to recognize the support from Paul McGinnity of the Radiological Protection Institute of Ireland in providing early access to monitoring data and critical comments regarding their interpretation.

References

Bowyer, T. W., S. R. Biegalski, M. Cooper, P. W. Eslinger, D. Haas, J. C. Hayes, H. S. Miley, D. J. Strom, and V. Woods (2011), Elevated radioxenon detected remotely following the Fukushima nuclear accident, *J. Environ. Radioact.*, *102*, 681–687, doi:10.1016/j.jenvrad.2011.04.009.

Chino, M., H. Nakayama, H. Nagai, H. Terada, G. Katata, and H. Yamazawa (2011), Preliminary estimation of release amounts of ^{131}I and ^{137}Cs accidentally discharged from the Fukushima Daiichi nuclear power plant into the atmosphere, *J. Nucl. Sci. Technol.*, *48*, 1129–1134, doi:10.3327/jnst.48.1129.

Cohen, M., et al. (2002), Modeling the atmospheric transport and deposition of PCDD/F to the Great Lakes, *Environ. Sci. Technol.*, *36*, 4831–4845, doi:10.1021/es0157292.

D'Amours, R., A. Malo, R. Servranckx, D. Bensimon, S. Trudel, and J.-P. Gauthier (2010), Application of the atmospheric Lagrangian particle dispersion model MLDP0 to the 2008 eruptions of Okmok and Kasatochi volcanoes, *J. Geophys. Res.*, *115*, D00L11, doi:10.1029/2009JD013602.

Draxler, R. R. (1999), HYSPLIT_4 user's guide, *NOAA Tech. Memo. ERL ARL-230*, 35 pp., Air Resour. Lab., Silver Spring, Md. [Available at http://www.arl.noaa.gov/documents/reports/hysplit_user_guide.pdf.]

Draxler, R. R., and J. L. Heffter (1981), Workbook for estimating the climatology of regional-continental scale atmospheric dispersion and deposition over the United States, *NOAA Tech. Memo. ERL ARL-96*, 25 pp., Air Resour. Lab., Silver Spring, Md.

Draxler, R. R., and G. D. Hess (1997), Description of the HYSPLIT_4 modeling system, *NOAA Tech. Memo. ERL ARL-224*, 24 pp., Air Resour. Lab., Silver Spring, Md.

Draxler, R. R., and G. D. Hess (1998), An overview of the HYSPLIT_4 modelling system for trajectories, dispersion, and deposition, *Aust. Meteorol. Mag.*, *47*, 295–308.

Draxler, R. R., M. Jean, B. Hicks, and D. Randerson (1997), Emergency preparedness—Regional specialized meteorological centers at Washington and Montréal, *Radiat. Prot. Dosimetry*, *73*(1–4), 27–30.

Hicks, B. B. (1986), Differences in wet and dry particle deposition parameters between North America and Europe, in *Aerosols: Research, Risk Assessment, and Control Strategies*, pp. 973–982, Lewis, Chelsea, Mich.

Jones, A., D. Thomson, M. Hort, and B. Devenish (2007), The U.K. Met Office's next generation atmospheric dispersion model, NAME III, in *Air Pollution Modeling and Its Application, Proceedings of the 27th NATO/CCMS International Technical Meeting on Air Pollution Modelling and Its Application*, vol. XVII, edited by C. Borrego and A.-L. Norman, pp. 580–589, Springer, New York.

Leon, J. D., D. A. Jaffe, J. Kaspar, A. Knecht, M. L. Miller, R. G. H. Robertson, and A. G. Schubert (2011), Arrival time and magnitude of airborne fission products from the Fukushima, Japan, reactor incident as measured in Seattle, WA, USA, *J. Environ. Radioact.*, *102*, 1032–1038, doi:10.1016/j.jenvrad.2011.06.005.

Lindberg, S. E. (1982), Factors influencing tracer metal, sulfate, and hydrogen ion concentrations in rain, *Atmos. Environ.*, *16*(7), 1701–1709, doi:10.1016/0004-6981(82)90263-3.

Lozano, R. L., M. A. Hernández-Ceballos, J. A. Adame, M. Casas-Ruíz, M. Sorribas, E. G. San Miguel, and J. P. Bolívar (2011), Radioactive impact of Fukushima accident on the Iberian Peninsula: Evolution and plume previous pathway, *Environ. Int.*, *37*, 1259–1264, doi:10.1016/j.envint. 2011.06.001.

Manolopoulou, M., E. Vagena, S. Stoulos, A. Ioannidou, and C. Papastefanou (2011), Radioiodine and radiocesium in Thessaloniki, northern Greece due to the Fukushima nuclear accident, *J. Environ. Radioact.*, *102*, 796–797, doi:10.1016/j.jenvrad.2011.04.010.

Masson, O., et al. (2011), Tracking of airborne radionuclides from the damaged Fukushima Daiichi nuclear reactors by European networks, *Environ. Sci. Technol.*, *45*, 7670–7677, dx.doi.org/10.1021/es2017158, doi:10.1021/es2017158.

Morino, Y., T. Ohara, and M. Nishizawa (2011), Atmospheric behavior, deposition, and budget of radioactive materials from the Fukushima Daiichi nuclear power plant in March 2011, *Geophys. Res. Lett.*, *38*, L00G11, doi:10.1029/2011GL048689.

Moyers, J. L., and R. A. Duce (1972), Gaseous and particulate iodine in the marine atmosphere, *J. Geophys. Res.*, *77*, 5229–5238, doi:10.1029/JC077i027p05229.

Seibert, P. (2000), Methods for source determination in the context of the CTBT radionuclide monitoring system, paper presented at Informal Workshop on Meteorological Modelling in Support of CTBT Verification, Univ. of Agric. Sci., Vienna, Dec. [Available at http://www.boku.ac.at/imp/iws-met-ver/PDF/SEIBERT/seibert1.pdf.]

Stohl, A., et al. (2011a), Determination of time- and height-resolved volcanic ash emissions and their use for quantitative ash dispersion modeling: The 2010 Eyjafjallajökull eruption, *Atmos. Chem. Phys.*, *11*, 4333–4351, doi:10.5194/acp-11-4333-2011.

Stohl, A., P. Seibert, G. Wotawa, D. Arnold, J. F. Burkhart, S. Eckhardt, C. Tapia, A. Vargas, and T. J. Yasunari (2011b), Xenon-133 and caesium-137 releases into the atmosphere from the Fukushima Daiichi nuclear power plant: Determination of the source term, atmospheric dispersion, and deposition, *Atmos. Chem. Phys. Discuss.*, *11*, 28,319–28,394, doi:10.5194/acpd-11-28319-2011.

World Meteorological Organization (WMO) (2006), Environmental emergency response: WMO activities, *WMO Bull. 55*, Geneva, Switzerland. [Available at ftp://ftp.wmo.int/Documents/PublicWeb/www/era/ERA-WMO_Bulletin_Jan2006.pdf.]

World Meteorological Organization (WMO) (2010), Manual on the global data processing and forecasting system, *WMO 485*, Geneva, Switzerland. [Available at http://www.wmo.int/pages/prog/www/DPFS/Manual_GDPFS.html.]

R. R. Draxler and G. D. Rolph, NOAA Air Resources Laboratory, 1315 East-West Hwy., Silver Spring, MD 20910, USA. (roland.draxler@noaa.gov)